

# STRESS FIELD MODEL FOR IMPACT DAMAGE EVALUATION IN COMPOSITES

Russell, S.\*

Aerospace Structures Engineer, Dallas, Texas, USA

\* Corresponding author ([sgrnd1983@gmail.com](mailto:sgrnd1983@gmail.com))

**Keywords:** *composites, impact damage, strength prediction*

## ABSTRACT

Damage evaluation in composite structures is one of the most persistent problems facing structural engineers in industry. The physics of damage initiation and evolution in composites is complex, involving multiple length scales and material failure modes. In recent years, computational structural mechanics methodologies have been developed to address some of this complexity, and further progress can be expected in the future. Initial damage assessments, however, require analytical models to make rapid structural integrity decisions for detail parts or assemblies. Stress field models covering a wide range of composite structural damage must be coupled with appropriate failure criteria to provide strength predictions.

This paper focuses on an elastic inclusion stress field model for composite impact damage. The elliptical shaped elastic inclusion, or region of reduced stiffness, is embedded in a two-dimensional, generally orthotropic composite plate subjected to remote in-plane stresses. The boundary value problem and solution by complex potential functions are discussed to facilitate application of the model. The paper also provides guidance for estimating stiffness reduction due to impact damage, since this is the primary damage parameter required to use the elastic inclusion model. Different approaches are offered based on the type of inspection data available for the damage. An example application is provided to illustrate predictive capability.

## 1 INTRODUCTION

Complex potential functions have been successfully used to solve numerous structural mechanics problems in composite aircraft structures design. The most commonly used approach has its roots in the pioneering work by Lekhnitskii over 50 years ago [1]. More recent developments have developed an alternate approach called the Stroh formalism [2], and this has resulted in complex potential formulations with greater generality and more desirable mathematical features. However, the vast majority of complex potential applications used in industry are based on Lekhnitskii complex potentials, which are widely used in the evaluation of cutouts, fastener holes, reduced stiffness zones known as inclusions, and large notches or cracks. Despite their widespread application, the derivations of important results are not as well-known as they should be. Lekhnitskii's original book is not widely available, and it sometimes omits details in the derivation of important results. This paper will attempt to address part of this knowledge gap by providing a general approach for evaluating an elliptical elastic inclusion, centrally located in an infinite elastic, generally orthotropic plate subjected to loading by uniform, remote in-plane stresses. This stress field model is suitable for evaluating the residual strength of composite laminated panels subjected to impact damage.

Several different investigators have developed the inclusion model for representing impact damage in composite laminates [3 – 5]. Most papers omit the details that would allow composite stress and damage tolerance analysts to implement the model in practice. This paper attempts to address this need, since analytical solutions of this kind are useful for establishing allowable damage limits for impact damage and supporting rapid damage assessments for aircraft in service.

\* Current Affiliation: Triumph Aerospace Structures, Arlington, Texas USA

## 2 STRESS FIELD MODEL

Lekhnitskii formulated a general approach to the solution of plate problems in anisotropic elasticity [1]. Infinitesimal deformations are assumed, leading to linear strain-displacement equations. In-plane stresses and strains are related by a linear, generally orthotropic stress-strain or constitutive relationship. Static equilibrium equations for the in-plane stress components are automatically satisfied by introduction of Airy's stress function [6]. The compatibility equation relating the infinitesimal strain and in-plane displacements can be reduced to a single fourth order linear partial differential equation for the unknown stress function. Lekhnitskii showed that the general solution to this partial differential equation can be expressed in terms of two complex valued potential functions. The solution of the plane stress linear elasticity problem for generally orthotropic plates is reduced to finding the complex potential functions satisfying the boundary conditions for specific problems.

Figure 1 shows the geometry of the elastic inclusion stress field model. The origin of coordinates for the analysis is located at the center of the elliptical inclusion. Lekhnitskii developed the complex potential solution for the stresses and strains in the inclusion, and in the plate outside the inclusion. For uniform remote stresses  $\sigma_x^o, \sigma_y^o, \tau_{xy}^o$ , the stresses  $f_x, f_y, f_{xy}$  in the inclusion are uniform. The inclusion stresses are obtained by solving four algebraic equations for  $f_x, f_y, f_{xy}$  and the relative rotation  $\Delta\omega$  of the inclusion with respect to the surrounding elastic plate. This solution is used in complex potential function formulae to calculate the stresses in the plate outside the inclusion.

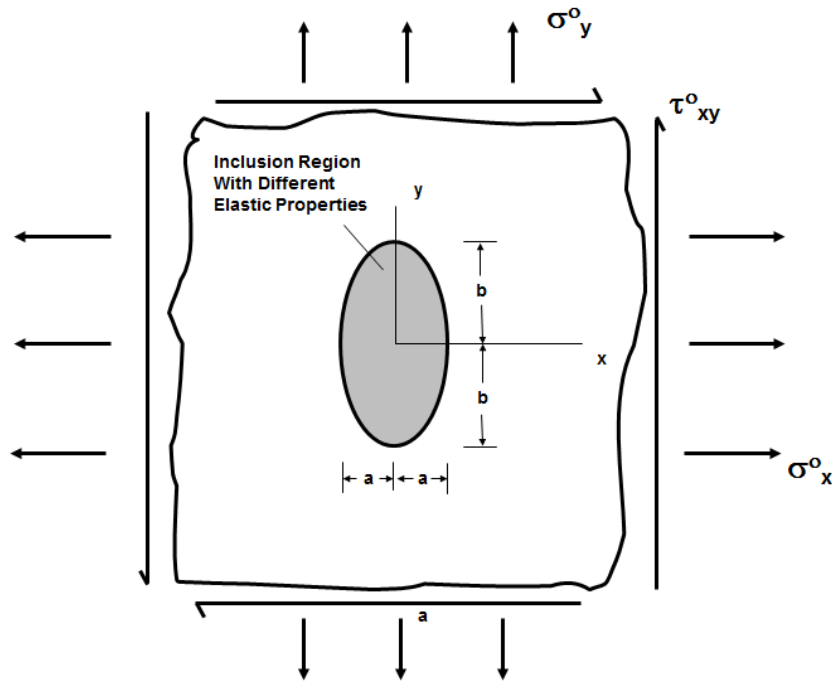


Figure 1: Elastic inclusion model for composite impact damage

### 2.1 Elastic Stress-Strain Relations

The relationship between in-plane stresses ( $\sigma_x, \sigma_y, \tau_{xy}$ ) and strains ( $\epsilon_x, \epsilon_y, \gamma_{xy}$ ) for a generally orthotropic plate can be written in the form:

$$\begin{aligned}
\varepsilon_x &= a_{11}\sigma_x + a_{12}\sigma_y + a_{16}\tau_{xy} \\
\varepsilon_y &= a_{12}\sigma_x + a_{22}\sigma_y + a_{26}\tau_{xy} \\
\gamma_{xy} &= a_{16}\sigma_x + a_{26}\sigma_y + a_{66}\tau_{xy}
\end{aligned} \tag{1}$$

where the  $a_{ij}$  ( $i, j = 1, 2$  or  $6$ ) are the elastic compliances of the plate material containing the inclusion. The elastic compliances  $a_{ij}$  are often written in a form using elastic moduli and Poisson's ratios for the laminated composite plate. In the inclusion region, the elastic compliances, stresses and strains differ from those of the parent plate material. The corresponding relationship between in-plane stresses ( $f_x, f_y, f_{xy}$ ) and in-plane strains ( $e_x, e_y, g_{xy}$ ) for the inclusion region is

$$\begin{aligned}
e_x &= a'_{11}f_x + a'_{12}f_y + a'_{16}f_{xy} \\
e_y &= a'_{12}f_x + a'_{22}f_y + a'_{26}f_{xy} \\
g_{xy} &= a'_{16}f_x + a'_{26}f_y + a'_{66}f_{xy}
\end{aligned} \tag{2}$$

where the  $a'_{ij}$  ( $i, j = 1, 2$  or  $6$ ) are the corresponding elastic compliances for the inclusion region. The elastic stiffnesses  $c_{ij}$  and  $c'_{ij}$  are the inverse of the elastic compliances  $a_{ij}$  and  $a'_{ij}$ , respectively. The solution presented in this paper is developed in terms of the elastic compliances.

## 2.2 Complex Potential Function Definitions

Lekhnitskii [1] reduces the elastic boundary value problem for the stresses in the generally orthotropic elastic plate containing the inclusion to the solution for two complex potential functions  $\Phi_1(z_1), \Phi_2(z_2)$ . The generalized complex variables  $z_1, z_2$  are defined by the relations  $z_1 = x + \mu_1 y, z_2 = x + \mu_2 y$  where  $\mu_1, \mu_2$  are roots of the characteristic polynomial equation that arises from the introduction of the Airy stress function into the strain compatibility equation for plane elasticity problems. The characteristic polynomial equation is

$$a_{11}\mu^4 - 2a_{16}\mu^3 + (2a_{12} + a_{66})\mu^2 - 2a_{26}\mu + a_{22} = 0 \tag{3}$$

The roots of the characteristic polynomial occur in complex conjugate pairs. Note that the complex conjugate quantities  $\bar{\mu}_1, \bar{\mu}_2$  are also roots. For the commonly encountered case where the generally orthotropic elastic plate is approximated as a specially orthotropic plate with elastic moduli and Poisson's ratio  $E_x, E_y, G_{xy}, \nu_{xy}$ , the roots of Eq. (1) can be written in closed form. Let

$$\chi = \frac{E_x}{2G_{xy}} - \nu_{xy}, \quad \lambda = \sqrt{\frac{E_x}{E_y}} \tag{4}$$

Then, if  $\chi \geq \lambda$ , the roots are purely imaginary and are of the form

$$\mu_1, \bar{\mu}_1 = \pm i\beta_1 \quad \mu_2, \bar{\mu}_2 = \pm i\beta_2 \tag{5}$$

$$\text{where} \quad \beta_1^2 = \chi - \sqrt{\chi^2 - \lambda^2}, \quad \beta_2^2 = \chi + \sqrt{\chi^2 - \lambda^2} \tag{6}$$

If  $\chi < \lambda$ , the roots are of the form

$$\mu_1, \bar{\mu}_1 = \alpha \pm i\beta \quad \mu_2, \bar{\mu}_2 = -\alpha \pm i\beta \tag{7}$$

$$\text{where} \quad \alpha = \text{Re}\left\{\left[-\chi + i\sqrt{\lambda^2 - \chi^2}\right]^{1/2}\right\}, \quad \beta = \text{Im}\left\{\left[-\chi + i\sqrt{\lambda^2 - \chi^2}\right]^{1/2}\right\} \tag{8}$$

and  $\text{Re}\{ \}$ ,  $\text{Im}\{ \}$  denote the real and imaginary parts of a complex quantity.

Stresses associated with the complex potential functions are given by

$$\begin{aligned}\sigma_x &= 2 \cdot \text{Re}[\mu_1^2 \Phi_1'(z_1) + \mu_2^2 \Phi_2'(z_2)] \\ \sigma_y &= 2 \text{Re}[\Phi_1'(z_1) + \Phi_2'(z_2)] \\ \tau_{xy} &= -2 \text{Re}[\mu_1 \Phi_1'(z_1) + \mu_2 \Phi_2'(z_2)]\end{aligned}\quad (9)$$

where the prime denotes differentiation with respect to the argument. The displacement solution is given by

$$u = 2 \text{Re}[p_1 \Phi_1(z_1) + p_2 \Phi_2(z_2)] - \omega y + u_o \quad (10)$$

$$v = 2 \text{Re}[q_1 \Phi_1(z_1) + q_2 \Phi_2(z_2)] + \omega x + v_o \quad (11)$$

where

$$p_j = a_{11} \mu_j^2 + a_{12} - a_{16} \mu_j \quad (12)$$

$$q_j = a_{12} \mu_j + \frac{a_{22}}{\mu_j} - a_{26} \quad (13)$$

and  $j = 1$  or  $2$ . The complex potential functions,  $\Phi_1(z_1)$ ,  $\Phi_2(z_2)$ , which automatically satisfy equilibrium and compatibility requirements, are formulated to satisfy the specific boundary conditions for a particular problem. For the elastic inclusion problem, these boundary conditions are (1) that the stress state at a large distance from the inclusion approaches the remote stress state  $\sigma_x^o$ ,  $\sigma_y^o$ ,  $\tau_{xy}^o$ , and (2) that continuity of tractions and displacements occurs at the interface between the inclusion and the parent plate material outside of the inclusion.

### 2.3 Solution of the Elastic Inclusion Boundary Value Problem

Lekhnitskii [1] noted that application of remote stresses to the elastic plate shown in Figure 1 produces uniform stresses  $f_x$ ,  $f_y$ ,  $f_{xy}$  in the elliptical elastic inclusion region. This result is not obvious, but it does lead to a solution that satisfies the required boundary conditions in the remote regions of the plate and at the elliptical interface between the inclusion and parent plate material. The stresses in the plate material, outside the inclusion region, are given by

$$\begin{aligned}\sigma_x &= \sigma_x^o + 2 \cdot \text{Re}[\mu_1^2 \Phi_1'(z_1) + \mu_2^2 \Phi_2'(z_2)] \\ \sigma_y &= \sigma_y^o + 2 \text{Re}[\Phi_1'(z_1) + \Phi_2'(z_2)] \\ \tau_{xy} &= \tau_{xy}^o - 2 \text{Re}[\mu_1 \Phi_1'(z_1) + \mu_2 \Phi_2'(z_2)]\end{aligned}\quad (14)$$

The boundary condition that the stresses reduce to the remote stress at large distances from the inclusion requires that  $\Phi_1(z_1)$ ,  $\Phi_2(z_2) \rightarrow 0$  as  $z_1, z_2 \rightarrow \infty$ .

The complex potential functions satisfying the boundary conditions along the elliptical interface between the inclusion and plate are of the form

$$\Phi_1(z_1) = \frac{A_1}{\zeta_1}, \quad \Phi_2(z_2) = \frac{B_1}{\zeta_2} \quad (15)$$

where  $A_l, B_l$  are complex constants to be determined and  $\zeta_l(z_l), \zeta_2(z_2)$  are functions that map the elliptical contour to a unit circle in the complex plane. For the elliptical contour, these functions are given in closed form by the equations

$$\zeta_l(z_l) = \frac{z_l \pm \sqrt{z_l^2 - (a^2 + \mu_l^2 b^2)}}{a - i\mu_l b}, \quad \zeta_2(z_2) = \frac{z_2 \pm \sqrt{z_2^2 - (a^2 + \mu_2^2 b^2)}}{a - i\mu_2 b} \quad (16)$$

where  $i^2 = -1$  and the sign of the square root is always chosen so that  $|\zeta_l(z_l)|, |\zeta_2(z_2)| > 1$ .

Surface tractions and displacements must be continuous across the interface between the inclusion and parent plate material. The boundary conditions for continuity of surface tractions can be expressed in the form

$$2 \operatorname{Re}[\Phi_l(z_l) + \Phi_2(z_2)] = Y_n = (f_y - \sigma_y^o)x - (f_{xy} - \tau_{xy}^o)y \quad (17)$$

$$2 \operatorname{Re}[\mu_l \Phi_l(z_l) + \mu_2 \Phi_2(z_2)] = -X_n = -(f_{xy} - \tau_{xy}^o)x + (f_x - \sigma_x^o)y \quad (18)$$

Note that  $x = a \cos \theta, y = b \sin \theta, \zeta_l = e^{i\theta}, \zeta_2 = e^{i\theta}$  on the inclusion interface, where  $\theta$  is an angular parameter that varies from 0 to  $2\pi$  for a complete circuit in the counterclockwise direction around the ellipse, and where  $a, b$  are the ellipse semi-axis lengths as shown in Figure 1. The surface traction continuity conditions in Equations (17) and (18) lead to solutions for the parameters  $A_l, B_l$  in Equation (15):

$$A_l = \frac{I}{2(\mu_l - \mu_2)} \left[ (f_x - \sigma_x^o)ib - (f_y - \sigma_y^o)\mu_2 a + (f_{xy} - \tau_{xy}^o)(i\mu_2 b - a) \right] \quad (19)$$

$$B_l = \frac{-I}{2(\mu_l - \mu_2)} \left[ (f_x - \sigma_x^o)ib - (f_y - \sigma_y^o)\mu_l a + (f_{xy} - \tau_{xy}^o)(i\mu_l b - a) \right] \quad (20)$$

The displacement solutions for the inclusion and surrounding plate material are obtained by first pinning the plate and inclusion at the origin. This condition makes the rigid body displacements  $u_o, v_o = 0$  in Eqs. (10) and (11). Then, the conditions of displacement continuity across the interface between the inclusion and parent plate material are applied to obtain the following equations:

$$\begin{aligned} & 2 \operatorname{Re}[p_1 \Phi_l(z_l) + p_2 \Phi_2(z_2)] + (a_{11}\sigma_x^o + a_{12}\sigma_y^o + a_{16}\tau_{xy}^o)x + \frac{1}{2}(a_{16}\sigma_x^o + a_{26}\sigma_y^o + a_{66}\tau_{xy}^o)y - \omega y \\ & = (a'_{11}f_x + a'_{12}f_y + a'_{16}f_{xy})x + \frac{1}{2}(a'_{16}f_x + a'_{26}f_y + a'_{66}f_{xy})y - \omega' y \end{aligned} \quad (21)$$

$$\begin{aligned} & 2 \operatorname{Re}[q_1 \Phi_l(z_l) + q_2 \Phi_2(z_2)] + (a_{12}\sigma_x^o + a_{22}\sigma_y^o + a_{26}\tau_{xy}^o)y + \frac{1}{2}(a_{16}\sigma_x^o + a_{26}\sigma_y^o + a_{66}\tau_{xy}^o)x + \omega x \\ & = (a'_{12}f_x + a'_{22}f_y + a'_{26}f_{xy})y + \frac{1}{2}(a'_{16}f_x + a'_{26}f_y + a'_{66}f_{xy})x + \omega' x \end{aligned} \quad (22)$$

where  $\omega, \omega'$  are the rigid body rotations in the parent plate material and inclusion, respectively. Substituting the complex potential solution from Eqs. (15), (16), (19) and (20) into Eqs. (21) and (22) and specializing the result for the interface contour, where  $x = a \cos \theta, y = b \sin \theta, \zeta_l = e^{i\theta}, \zeta_2 = e^{i\theta}$  leads to four linear algebraic equations to be solved for the unknown inclusion stresses  $f_x, f_y, f_{xy}$  and the relative rigid body rotation  $\Delta\omega = \omega' - \omega$  between the inclusion and parent plate material. With this solution, the stresses in the plate outside the inclusion can be calculated from Eqs. (14), (15), (19) and (20).

The four linear algebraic equations to be solved for the inclusion stresses and relative rigid body rotation are the following two complex algebraic equations and their complex conjugates:

$$\begin{aligned} & \left[ i \frac{(p_1 - p_2)}{(\mu_1 - \mu_2)} b - a'_{11} a - \frac{1}{2} i a'_{16} b \right] f_x + \left[ \frac{(\mu_1 p_2 - \mu_2 p_1)}{(\mu_1 - \mu_2)} a - a'_{12} a - \frac{1}{2} i a'_{26} b \right] f_y \\ & + \left[ \frac{-(p_1 - p_2) a}{(\mu_1 - \mu_2)} + \frac{i(\mu_2 p_1 - \mu_1 p_2) b}{(\mu_1 - \mu_2)} - a'_{16} a - \frac{1}{2} i a'_{66} b \right] f_{xy} + i \Delta \omega b = \end{aligned} \quad (23)$$

$$\begin{aligned} & \left[ i \frac{(p_1 - p_2)}{(\mu_1 - \mu_2)} b - a'_{11} a - \frac{1}{2} i a'_{16} b \right] \sigma_x^o + \left[ \frac{(\mu_1 p_2 - \mu_2 p_1)}{(\mu_1 - \mu_2)} a - a'_{12} a - \frac{1}{2} i a'_{26} b \right] \sigma_y^o \\ & + \left[ \frac{-(p_1 - p_2) a}{(\mu_1 - \mu_2)} + \frac{i(\mu_2 p_1 - \mu_1 p_2) b}{(\mu_1 - \mu_2)} - a'_{16} a - \frac{1}{2} i a'_{66} b \right] \tau_{xy}^o \end{aligned}$$

$$\begin{aligned} & \left[ i \frac{(q_1 - q_2)}{(\mu_1 - \mu_2)} b - i a'_{12} b - \frac{1}{2} a'_{16} a \right] f_x + \left[ \frac{(\mu_1 q_2 - \mu_2 q_1)}{(\mu_1 - \mu_2)} a - i a'_{22} b - \frac{1}{2} a'_{26} a \right] f_y \\ & + \left[ \frac{-(q_1 - q_2) a}{(\mu_1 - \mu_2)} + \frac{i(\mu_2 q_1 - \mu_1 q_2) b}{(\mu_1 - \mu_2)} - i a'_{26} b - \frac{1}{2} a'_{66} a \right] f_{xy} - \Delta \omega a = \end{aligned} \quad (24)$$

$$\begin{aligned} & \left[ i \frac{(q_1 - q_2)}{(\mu_1 - \mu_2)} b - i a'_{12} b - \frac{1}{2} a'_{16} a \right] \sigma_x^o + \left[ \frac{(\mu_1 q_2 - \mu_2 q_1)}{(\mu_1 - \mu_2)} a - i a'_{22} b - \frac{1}{2} a'_{26} a \right] \sigma_y^o \\ & + \left[ \frac{-(q_1 - q_2) a}{(\mu_1 - \mu_2)} + \frac{i(\mu_2 q_1 - \mu_1 q_2) b}{(\mu_1 - \mu_2)} - i a'_{26} b - \frac{1}{2} a'_{66} a \right] \tau_{xy}^o \end{aligned}$$

Note that when there is no difference in elastic properties between the inclusion and parent plate material, i.e.  $a'_{ij} = a_{ij}$  ( $i, j = 1, 2$  or  $6$ ), the trivial solution is obtained where  $f_x = \sigma_x^o$ ,  $f_y = \sigma_y^o$ , and  $\Delta \omega = 0$ . Conversely, when the elastic stiffness  $a'_{ij} \rightarrow 0$ , the complex potential function solution in Eqs. (15), (16), (19) and (20) reduces to the solution for an elliptical cutout in an infinite plate loaded by remote in-plane stresses.

### 3 EXAMPLE STRESS FIELD SOLUTIONS

The utility of any stress field model for damaged material lies in its ability to predict gradients of stresses and strains in the vicinity of the damage. Failure criteria developed for the notched strength of composite laminates, such as the point stress criterion and average stress criterion [7] require this type of detail for the stress field. These failure criteria are widely used to calculate residual strength of composite laminated plates containing stress-raisers such as cutouts, impact damage and cracks [8].

Figures 2 and 3 show an example calculation obtained using the stress field model presented in Section 2. The example considers an elliptical shaped inclusion similar to the geometry shown in Figure 1 in a 24 ply laminate constructed from IM7/8552 material. The material ply-level elastic constants [9] are  $E_1 = 162138$  MPa,  $E_2 = 9724$  MPa,  $G_{12} = 4690$  MPa, and  $\nu_{12} = 0.316$ , where '1' denotes the fiber direction and '2' the direction transverse to the fibers. The cured ply thickness is  $t_{ply} = 0.183$  mm. Two different 24-ply laminates are considered to illustrate the range of material response that can be expected: a 'hard' laminate with (50/33/17) construction, i.e. 50%  $0^\circ$  plies, 33%  $\pm 45^\circ$  plies, 17%  $90^\circ$  plies; and a 'soft' laminate with (17/66/17) construction. The inclusion in this example has an aspect ratio of  $b/a = 4$ . Figure 2 illustrates the variation of the tangential stress component along the inclusion boundary for the case where remote tension stress  $\sigma_x^o = 100$

MPa. The influence of the inclusion stiffness reduction can be seen from the results, which are shown for cases of 25%, 75% and 100% stiffness reduction, the latter case representing an open hole. Note the large gradient of tangential stress around the inclusion interface, and the peak stress concentration along the major axes of the ellipse. The hard laminate has a sharp peak and severe stress concentration which increases in magnitude as the stiffness reduction of the inclusion increases. The soft laminate exhibits a similar trend, although the peaks of the stress variation are less severe. In both cases, retention of even a small amount of stiffness in the inclusion is sufficient to greatly reduce the severity of the peak stress concentration (e.g. compare the results for 75% and 100% stiffness reduction).

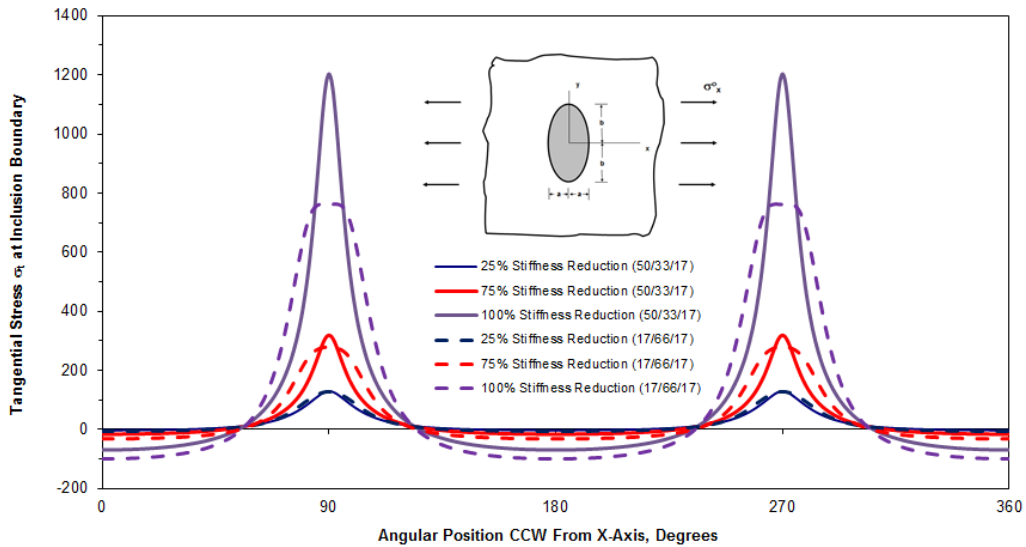


Figure 2: Tangential stress at elliptical inclusions in hard and soft laminates under remote tension stress

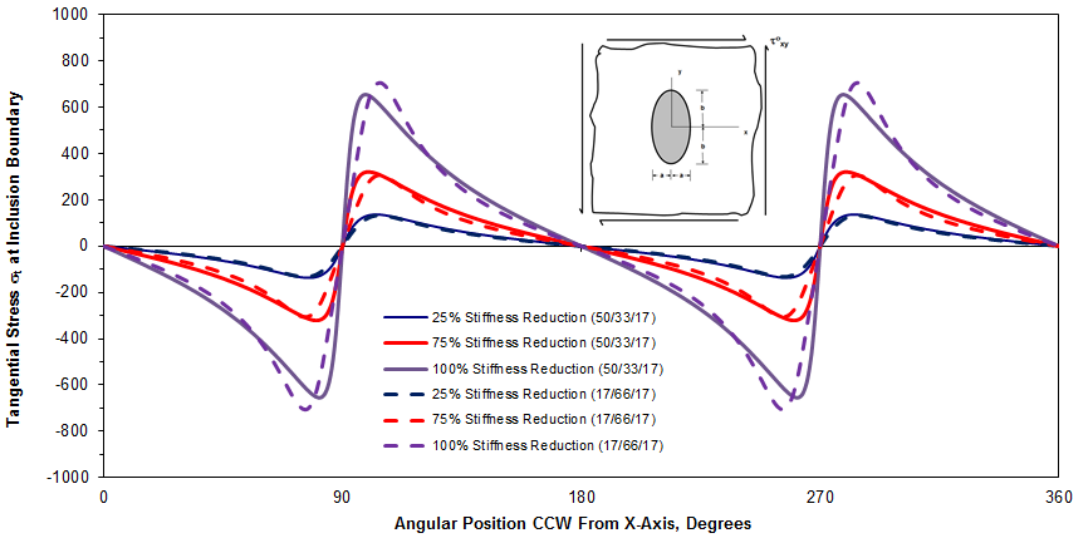


Figure 3: Tangential stress at elliptical inclusions in hard and soft laminates under remote shear stress

Figure 3 shows the tangential stress variation at the elliptical inclusion interface for the case of remote shear stress  $\tau_{xy}^0 = 100$  MPa applied to the laminate. The tangential stress variation is completely different for this case, but the effect of the inclusion stiffness is similar. Even small levels of residual stiffness in the inclusion region result in substantially reduced peak stress concentrations.

The example calculations shown in Figures 2 and 3 illustrate the sharp stress concentrations and large stress gradients that can exist near an elastic inclusion. The elastic inclusion with its reduced stiffness represents impact damage in the proposed stress field model. Accurately predicting stress concentration and stress gradient effects is crucial for generating damaged residual strength predictions with this type of model. A further requirement is successfully estimating stiffness reduction associated with impact damage.

#### 4 STIFFNESS REDUCTION AND FAILURE ESTIMATES

Impact of hard objects on composite laminates causes damage that increases with the energy level of the impact. In conventional laminated plates fabricated from unidirectional tape material, this damage is manifested as matrix cracks, broken fibers and delaminations. Each of these damage modes contributes to stiffness reduction in the laminate. Reliable methods of estimating the stiffness reduction are needed to successfully implement the inclusion stress field model described here.

A quick first estimate of stiffness reduction, applicable for cases where no detailed non-destructive inspection (NDI) data is available for the damage, is based on the dent depth produced by the impact event. Assume that (1) the impact event causes fiber breakage, matrix microcracking and delamination within the sublaminates thickness defined by the dent depth, and (2) the sublaminates defined by the dent depth is ineffective in transferring load due to this damage. With these assumptions, the reduced elastic stiffnesses in the impact zone can be estimated as

$$c'_{ij} / c_{ij} = (t_{incl} / t)^3 \quad (25)$$

where  $c_{ij}$ ,  $c'_{ij}$  are the elastic stiffnesses defined following Eq. (2),  $t_{incl}$  is the inclusion thickness (laminate thickness minus the dent depth) and  $t$  is the parent laminate thickness. This approach has been successfully used to provide estimates of compression after impact strength of laminates fabricated from several different material systems [10].

A more refined approach, applicable when NDI data is available for the damage region, is based on the rule of mixtures approach developed by O'Brien [11]. The rule of mixtures approach assumes that delamination is the dominant damage mode in the laminate. Consider the effect of the delaminations on the extensional stiffnesses  $A_{ij}$  of the laminate. For a delaminated laminate with  $M$  delaminations, the delaminations will divide the laminate into  $M + 1$  ply groups. The extensional stiffnesses  $A^k_{ij}$  can be calculated for each of these ply groups or sublaminates. By the rule of mixtures approach, the extensional stiffnesses  $A'_{ij}$  for the total laminate with  $M$  delaminations will be

$$A'_{ij} = \frac{\sum_{k=1}^{M+1} (A^k_{ij}) \cdot t_k}{\sum_{k=1}^{M+1} t_k} = \frac{1}{t} \cdot \sum_{k=1}^{M+1} (A^k_{ij}) \cdot t_k \quad (26)$$

This result can be used to calculate the elastic compliances  $a'_{ij}$  in the inclusion region of the stress field model.

As an example of the rule of mixtures approach, consider the hard (50/33/17) laminate evaluated in the stress field calculations shown in Figures 2 and 3. The laminate stacking sequence is  $[\pm 45/0_2/90/0_2/\pm 45/0_2/90]_s$ . For this example, suppose that an impact event causes a single delamination along the laminate mid-surface, producing two 12-ply sublaminates, and that the delamination is of an elliptical shape with  $a = 1$  cm and  $b = 4$  cm. Eq. (26) predicts a 50% reduction in the laminate stiffness in this damage zone due to the single delamination. Figure 4 shows the gradient of stresses produced by the reduced stiffness in the elliptical

inclusion region associated with the delamination. For a remote applied stress of  $\sigma_x^o = 100$  MPa, the normal stress  $\sigma_x$  along the y-axis coincident with the major axis of the elliptical inclusion is 184 MPa at the inclusion boundary. This normal stress drops off rapidly with distance from the inclusion boundary and approaches the remote value of  $\sigma_x^o = 100$  MPa at a distance of  $b = 4$  cm from the damage.

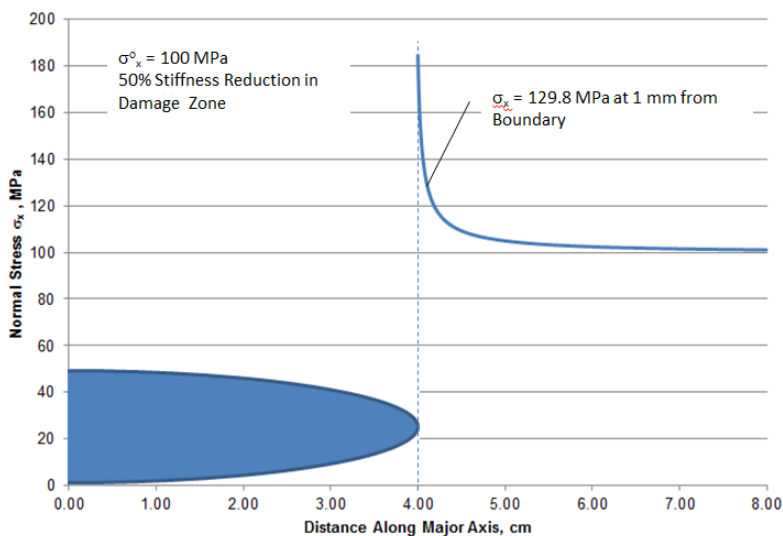


Figure 4: Stress concentration and gradient near elliptical inclusion, remote tension stress

Figure 4 also shows how a failure criterion can be used to estimate residual strength due to the impact damage. For the IM7/8552 material system in this example, the unnotched laminate strength is estimated to be  $F_x = 1497$  MPa. For simplicity, consider the point stress criterion with characteristic material distance of  $d_o = 1$  mm from the inclusion boundary. The stress  $\sigma_x = 129.8$  MPa at this location. Failure is hypothesized to occur when the remote applied stress causes the local stress at the characteristic material distance to equal  $F_x$ . Since the material response is assumed to be linearly elastic to failure, the failure stress for the damaged laminate is estimated to be  $F_{x,d} = 1153$  MPa, a strength reduction of 23% due to the damage. This particular example serves as an illustration; obviously more elaborate failure criteria can be used to generate refined failure estimates. Note that even light damage in the form of a single delamination at the laminate mid-plane results in a significant strength reduction.

## 5 SUMMARY

This paper presents the complete solution for the stress field model of an elliptical shaped elastic inclusion embedded in a generally orthotropic elastic plate under remote applied stress. The plate is infinite in extent, and hence suitable for cases where the inclusion is much smaller than the plate dimensions. The inclusion is a region of reduced elastic stiffness, which makes it a suitable model for impact damage in composites. The boundary value problem is presented in sufficient detail to allow engineers and researchers to implement the model using commonly available mathematical software packages.

Example calculations have been provided to illustrate the basic features of the model. The elliptical shaped inclusion generates stress concentrations that increase in severity with magnitude of the stiffness reduction due to the impact damage. The magnitude and location of the peak stress concentration depends upon the laminate ply content and remote applied stresses. Example calculations show that the stress field near the inclusion is characterized by large stress gradients. Accurately calculating these stresses and their gradients is essential for generating accurate failure estimates.

Two methods have been presented for estimating the stiffness reduction in the inclusion region due to impact damage. One method, based on visible dent depth, is very approximate and is suitable for usage when no other inspection data are available. A second method, based on the rule of mixtures [11], is based on calculating extensional stiffness reduction due to delaminations in the impact damage region. It is suitable for usage when NDI data is available to characterize the damage. An example calculation is provided to illustrate the application of the rule of mixtures approach, and the calculation of residual strength using a common failure criterion used for composite laminates with stress concentrations.

## 6 REFERENCES

- [1] S. Lekhnitskii. *Anisotropic plates*. Second edition, S. Tsai, T. Cheron translation, Gordon and Breach Science Publishers, 1968.
- [2] A. Stroh. Steady state problems in anisotropic elasticity. *Journal of Mathematical Physics*, Vol. 41, pp. 77-103, 1962.
- [3] D. Cairns, P. Lagace. Residual tensile strength of graphite/epoxy and Kevlar/epoxy laminates with impact damage. *Composite materials: testing and design (ninth volume)*. ASTM STP 1059, S. Garbo, ed., American Society for Testing and Materials, pp. 48-63, 1990.
- [4] Y. Xiong, C. Poon, P. Straznicki, H. Vietinghoff. A prediction method for the compressive strength of impact-damaged composite laminates. *Composite Structures*, 1995, Vol. 30, No.4, pp. 357-367, 1995.
- [5] B. Qi, I. Herszberg. An engineering approach for predicting residual strength of carbon/epoxy laminates after impact and hygrothermal cycling. *Composite Structures*, Vol. 47, No.1, pp. 483-490, 1999.
- [6] S. Timoshenko, J. Goodier. *Theory of elasticity*. 3rd edition, McGraw-Hill Book Company, 1970.
- [7] J. Whitney, R. Nuismer. Stress fracture criteria for laminated composites containing stress concentrations. *Journal of Composite Materials*, Vol. 8, pp. 253-265, 1974.
- [8] E. Barbero. *Introduction to composite materials design*. CRC Press, 1999.
- [9] K. Marlett. Hexcel 8552 IM7 unidirectional prepreg 190 gsm and 35% RC qualification material property data report. NCAMP Test Report CAM-RP-2009-015, Rev. A, Wichita State University, 2011.
- [10] S. Russell. A simplified progressive failure prediction model for impact-damaged composite structures. *Proceedings of 49th AIAA/ASME/ASCE/AHS/ASC Structures, Structural Dynamics and Materials Conference*, Schaumburg, Illinois USA, Paper AIAA-2008-2320, 2008.
- [11] T. O'Brien. Characterization of delamination onset and growth in a composite laminate. *NASA Technical Memorandum 81940*, 1981.